Structural analysis of the β-SiC(100)-c(2×2) surface reconstruction by automated tensor low-energy electron diffraction

J. M. Powers, A. Wander, P. J. Rous,* M. A. Van Hove, and G. A. Somorjai

*Materials Sciences Division, Center for Advanced Materials, Lawrence Berkeley Laboratory,
University of California, Berkeley, California 94720
and Department of Chemistry, University of California, Berkeley, California 94720*

(Received 6 March 1991)

The atomic structure of the β-SiC(100)-c(2×2) surface was analyzed using dynamical calculations of low-energy electron-diffraction intensities. The c(2×2) surface was prepared in ultrahigh vacuum by two different methods. The first utilized the removal of surface silicon by high-temperature annealing in ultrahigh vacuum. The second route utilized the deposition of surface carbon by exposing the stoichiometric (2×1) surface at 1125 K to C_2H_4. Our results showed that both methods produced a surface terminated with C_2 groups in staggered silicon bridge sites. Weak silicon dimer bonds were found in the second atomic layer of the c(2×2) surface produced by silicon sublimation, but not for the c(2×2) surface produced by C_2H_4 exposure. We postulate that hydrogen, released by the thermal decomposition of C_2H_4, saturated silicon dangling bonds in the second atomic layer, suppressing dimer formation.

I. INTRODUCTION

β-phase silicon carbide has received considerable attention recently as research has been directed towards understanding semiconductors capable of withstanding high temperatures and harsh environments.[1-3] A ceramic semiconductor, β-SiC possesses a large band-gap energy (2.3 eV) and can be doped both p and n type. Its chemical inertness, especially towards oxidation, makes it a promising candidate for high-temperature electronic applications.

Surface-science studies have shown that β-SiC, like GaAs, exhibits a wide range of surface reconstructions which are dependent on the surface composition.[4] The stoichiometric β-SiC(100) surface appears to be terminated in a layer of silicon atoms, which reconstruct to produce a (2×1) LEED pattern. This (2×1) reconstruction is believed to be analogous to the Si(100)-(2×1) surface, in which the topmost silicon atoms dimerize in order to reduce the number of unsaturated surface bonds. The addition of silicon to the stoichiometric β-SiC(100)-(2×1) surface has been reported to produce (3×2) and (5×2) surface reconstructions.[5] It is postulated that these surfaces involve rows of silicon dimers on top of a silicon terminated surface.

Several researchers have reported that high-temperature annealing of the β-SiC(100)-(2×1) surface produces a surface reconstruction exhibiting a c(2×2) LEED pattern.[6-8] To the best of our knowledge, no analogous structure has been reported for GaAs(100), Si(100), or diamond C(100). The ideal silicon-terminated unreconstructed β-SiC(100)-(1×1) surface is illustrated in Fig. 1(a). A variety of surface reconstruction models has been proposed for the β-SiC(100)-c(2×2) surface. Dayan proposed that the c(2×2) surface is terminated in a complete layer of silicon, with silicon dimers arranged in a staggered pattern,[8] as shown in Fig. 1(b). Kaplan,

believing the surface to be silicon deficient relative to the (2×1) reconstruction, proposed that the surface is terminated in 0.5 monolayer (ML) of silicon atoms.[4] These silicon atoms lie in the plane of the surface carbon atoms, positioned in alternating carbon hollow sites [Fig. 1(c)]. Based on medium energy ion scattering (MEIS) results, Hara et al. proposed that the c(2×2) surface is terminated in a complete monolayer of carbon.[5] However, a more detailed surface structure analysis was not reported.

Determining the c(2×2) surface structure using Auger-electron spectroscopy (AES) or MEIS is hampered by the fact that several of the possible β-SiC(100) reconstructions can exist on the surface simultaneously, dependent only on the local atomic composition. When this is the case, AES and MEIS sample multiple reconstructions simultaneously, due to the relatively large analysis areas of the techniques.

We have utilized LEED intensity-voltage (I-V) analysis to study the β-SiC(100)-c(2×2) surface structure. LEED is less sensitive to multiple surface reconstructions, since coherent scattering from these regions demands a relatively large domain size. The LEED pattern shows no evidence of fractional order beams from reconstructions with different superlattice unit cells, and hence, the problems encountered in the AES and MEIS studies are not present in this work.

Two different routes were utilized to prepare the c(2×2) surface reconstruction. As previously mentioned, annealing the (2×1) surface above 1300 K removes surface silicon via sublimation, producing a slightly diffuse c(2×2) pattern. Secondly, a sharper c(2×2) pattern may be obtained by the deposition of surface carbon, produced by exposing the (2×1) surface at 1125 K to ethylene (C_2H_4) gas. A comparison of the LEED I-V curves of both c(2×2) surfaces showed them to share many features, but with some clear differences. Our structural analysis indicated that both c(2×2) surfaces

were terminated with C_2 groups in staggered silicon bridge sites. Evidence of weak silicon dimer bond formation in the second atomic layer was found for the $c(2\times2)$ surface produced by silicon sublimation, but not for the $c(2\times2)$ surface produced by C_2H_4 exposure. This suggests that hydrogen, released by the thermal decomposition of C_2H_4, saturated silicon dangling bonds and suppressed silicon dimer formation.

II. EXPERIMENT

A Varian UHV system with a base pressure of 5×10^{-10} Torr was utilized for the AES and LEED studies. A PHI single pass cylindrical mirror analyzer was utilized for AES with a primary beam energy of 1.5 kV. A PHI four-grid LEED-Auger optics system was utilized for the LEED studies.
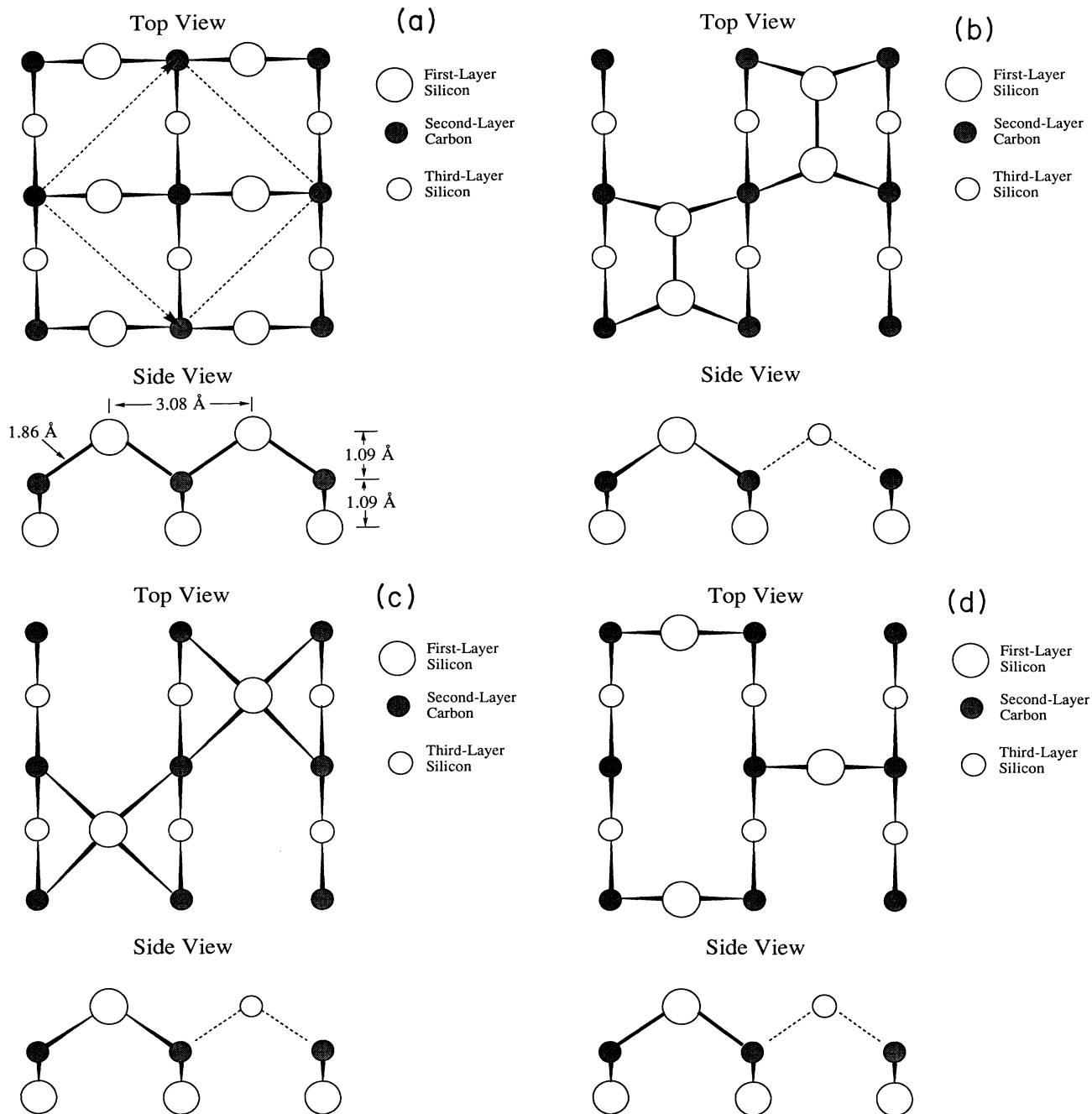

FIG. 1. Silicon-terminated models for the β-SiC(100)-(1×1) and $-c(2\times2)$ surfaces: (a) the ideal unreconstructed (1×1) surface with a superimposed $c(2\times2)$ unit cell, (b) the staggered Si dimer model, (c) Si in C hollow sites, and (d) Si in C bridge sites.

The β-SiC(100) samples utilized were 4–6-μm-thick films grown on Si(100) wafers via chemical vapor deposition. The samples were provided by Matus of NASA Lewis Research Center.[9] Previous research has shown that these films yield LEED patterns which are superpositions of patterns originating from surface domains rotated 90° relative to each other.[1] To generate a larger experimental data base (unaffected by domain averaging) a single-domain pattern is preferable. Thus, our studies utilized β-SiC(100) films grown on Si(100) wafers cut 0.5° towards the (110) direction. These off-normal β-SiC(100) films exhibited only 1-domain LEED patterns. The samples were mounted on an off-axis manipulator capable of independent azimuthal rotation. The samples were resistively heated using a constant current power supply. The removal of oxide from the β-SiC surface was performed *in situ* by heating the sample to 1175 K and placing it 2.5 cm from a resistively heated 2-cm^2 silicon wafer at approximately 1300 K. The flux of silicon atoms obtained from the silicon wafer removed the oxide from the β-SiC surface as $SiO_{(g)}$ and also allowed the surface silicon/carbon ratio to be controlled.

Two different techniques were utilized to produce the c(2$\times$2) surfaces. The first required the removal of surface silicon from a (2$\times$1) or (3$\times$2) surface by high-temperature annealing in UHV. At approximately 1300 K, the (2$\times$1) to c(2$\times$2) conversion required 10–15 min

of annealing, while a (3$\times$2) surface required an additional 5–10 min. A better ordered c(2$\times$2) surface could be produced by exposure of the (2$\times$1) surface at 1125 K to 100 L of C_2H_4 (1 langmuir = 10^{-6} Torr sec). Exposure of this c(2$\times$2) to additional C_2H_4 produced no change in the LEED pattern or the AES spectra.

The LEED data were collected using a silicon-intensified-target video camera. The video signal was digitized utilizing a video conversion board mounted in an Everex 386 PC, which was also used for data storage. The LEED I-V curves were then generated from the stored diffraction images. The LEED data were taken at normal incidence between 30 and 230 eV, in 2 eV increments. At each energy, 125 video images were averaged to increase the signal-to-noise ratio. The I-V curves of symmetrically equivalent beams were compared to check for normal incidence. Eight independent diffraction beams were analyzed for the c(2$\times$2) produced by C_2H_4 exposure. The cumulative energy range for the (0,1), (1,0), (1,1), (2,0), (0,2), ($\frac{1}{2},\frac{1}{2}$), ($\frac{3}{2},\frac{1}{2}$), and ($\frac{1}{2},\frac{3}{2}$) beams was 870 eV. Due to the lower quality of the c(2$\times$2) produced by silicon sublimation, only seven independent diffraction beams [(0,1), (1,0), (1,1), (2,0), ($\frac{1}{2},\frac{1}{2}$), ($\frac{1}{2},\frac{3}{2}$) and ($\frac{3}{2},\frac{1}{2}$)] were utilized. These seven beams had a cumulative energy range of 818 eV. The I-V curves due to the two preparation methods are compared in Figs. 2 and 3.
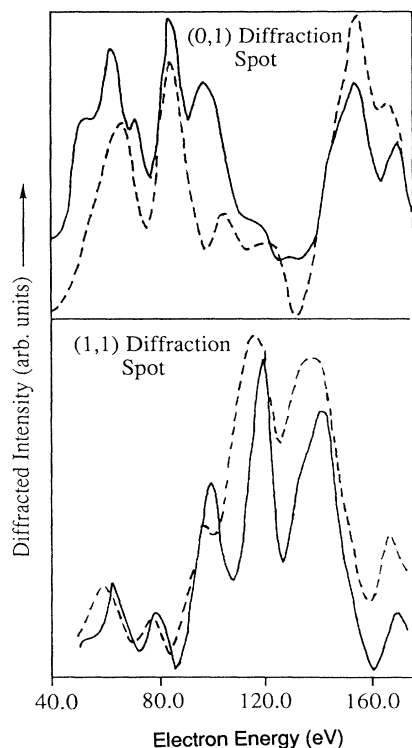

FIG. 2. The I-V curves of the (0,1) and (1,1) beams of the c(2$\times$2) structure produced by Si sublimation (solid line) and C_2H_4 exposure (dashed line).
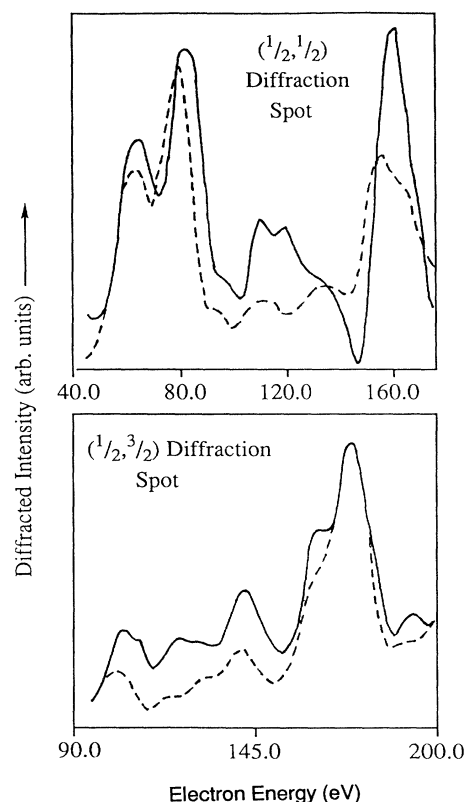

FIG. 3. The I-V curves of the ($\frac{1}{2},\frac{1}{2}$) and ($\frac{1}{2},\frac{3}{2}$) beams of the c(2$\times$2) structure produced by Si sublimation (solid line) and C_2H_4 exposure (dashed line).

III. LEED ANALYSIS

The experimental I-V curves were analyzed in two stages. First, a conventional dynamical LEED analysis was performed, in which only first-layer reconstruction was allowed, keeping the bulk structure in deeper layers. This enabled us to identify the most promising candidate structures for further analysis. The analysis of the best candidate structures was then refined by allowing any first- and second-layer relaxations to occur which were compatible with the $c(2\times2)$ periodicity. This analysis was performed using our recently developed automated search method based on tensor LEED (TLEED).[10]

The initial calculations were performed using standard dynamical LEED theory.[11] Phase shifts for silicon and carbon were derived from an infinite bulk lattice calcula-
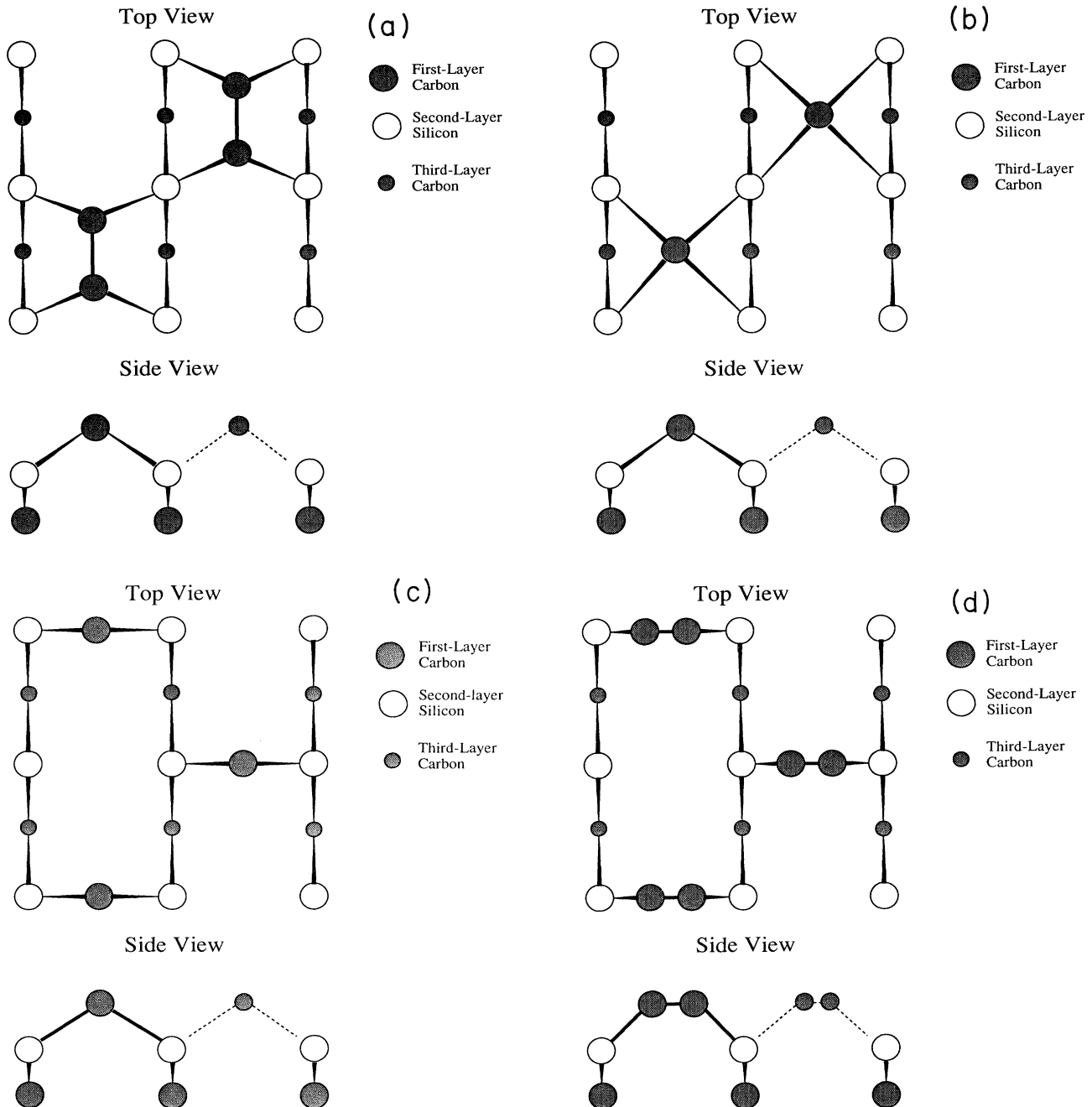

FIG. 4. Carbon-terminated trial models for the β-SiC(100)-$c(2\times2)$ surface: (a) the staggered C dimer model, (b) C in Si hollow sites, (c) C in Si bridge sites, and (d) C_2 groups in Si bridge sites.

tion using Herman-Skillman wave functions. A composite layer consisting of the first and second atomic layers was treated using matrix inversion, although only the first atomic layer was allowed to reconstruct. The use of a composite layer allows for possible small first- to second-layer distances. The layers were then stacked using layer doubling. Surface vibrations were included via a Debye-Waller factor. A Debye temperature equal to the bulk Debye temperature of 1430 K was used throughout both the dynamical and tensor LEED calculations. A damping term of -5 eV was used during this stage. The theoretical and experimental I-V curves were then compared using the Pendry R factor.

The analysis by tensor LEED allowed the atoms in the first and second layers to move independently in all three dimensions. Thus, 12 structural parameters were optimized simultaneously, in addition to the muffin-tin zero. This method utilizes first-order perturbation theory to express the change in amplitude of the scattered LEED intensities resulting from small displacements of the surface atoms. The first step in the method performs a dynamical LEED calculation for a reference structure. In addition, we evaluate the expansion coefficients for the perturbation series in the form of a tensor. In the second step, we use this tensor to perform a fast and efficient perturbative LEED calculation. This step is coupled with an optimization routine that allows us to quickly locate an R-factor minimum in structural parameter space. This method has previously been applied to the Mo(100)-c(2×2)-S (Ref. 12) and Rh(111)-(2×2)-C_2H_3 (Ref. 13) systems.

The TLEED method currently requires layer stacking to be performed using renormalized forward scattering. However, convergence problems were experienced using this technique together with the -5-eV damping term used in the conventional dynamical calculations. These problems were removed by increasing the damping to -6 eV. While this results in a broadening of the peaks in the theoretical I-V spectra, it should not significantly affect the structural outcome.

IV. STRUCTURAL MODELS EXAMINED

Seven different models were analyzed for the c(2×2) surface. In addition to the two models discussed previously [Figs. 1(b) and 1(c)], we examined a surface terminated with silicon atoms in staggered carbon bridge sites [Fig. 1(d)]. Based on the MEIS results of Hara et al., we also examined the carbon-terminated analogs of these models: (1) a surface terminated with staggered carbon dimers [Fig. 4(a)], (2) carbon atoms in silicon hollows [Fig. 4(b)], and (3) carbon atoms in silicon bridges [Fig. 4(c)]. Lastly, based on the reported adsorbed state of C_2H_4 on Si(100),[14] we examined a surface with C_2 groups in silicon bridging sites [Fig. 4(d)].

V. RESULTS AND DISCUSSION

According to AES, the atomic compositions of the c(2×2) surfaces produced by silicon sublimation or by C_2H_4 exposure were very similar (Fig. 5). As Fig. 5 shows, the c(2×2) surfaces exhibited a lower Si/C AES

ratio than the (2×1) surface. Assuming the (2×1) surface to be analogous to the Si(100)-(2×1) surface, the AES results indicated that the topmost atomic layer of the c(2×2) surface was either a mixed Si/C layer or was composed entirely of carbon atoms.

The results of the theoretical fitting of the I-V curves using the conventional dynamical LEED analysis are shown in Table I. These calculations clearly favored the model in which C_2 groups bridge silicon atoms. The muffin-tin zero for this model optimized at -10 ± 1 eV. A qualitatively similar model has been reported for C_2H_4 adsorbed on the Si(100)-(2×1) surface, in which the C_2H_4 molecule bonds on the silicon dimer, maintaining the (2×1) surface symmetry.[14] In addition, our model agrees with the MEIS results of Hara et al., since the terminating atomic layer of the model consists of a monolayer of carbon.[5]

Several characteristics of the c(2×2) surface support our preferred model. First, exposure of the (2×1) surface to C_2H_4 at elevated temperatures does not produce a c(2×2) pattern, implying a C—C surface bond is necessary to create the c(2×2) reconstruction. Secondly, the oxidation rate of the c(2×2) surface is lower than that of the (2×1) and (3×2) surfaces.[15] Previous research has shown that the rate of oxidation increases with increasing surface silicon concentration.[16] Our preferred model, in which the topmost atomic layer is only carbon, would not be expected to oxidize quickly. Lastly, exposure of the c(2×2) surface to H_2 does not change the LEED pattern symmetry, suggesting that the c(2×2) structure is not created by staggered silicon dimers. The (2×1) surface is readily converted to a (1×1) surface by exposure to 10^{-6} Torr of H_2 at 1125 K, indicating that H_2 exposure dissociates silicon dimers.

Based on the conventional dynamical LEED results, only the staggered carbon dimer and bridging C_2 groups models were further refined using tensor LEED. Once again, the calculations favored the C_2 bridging model, as shown in Table II. However, by allowing second-layer relaxations it was determined that the c(2×2) surface produced by C_2H_4 exposure was slightly different than the one produced by Si sublimation. For the surface pro-
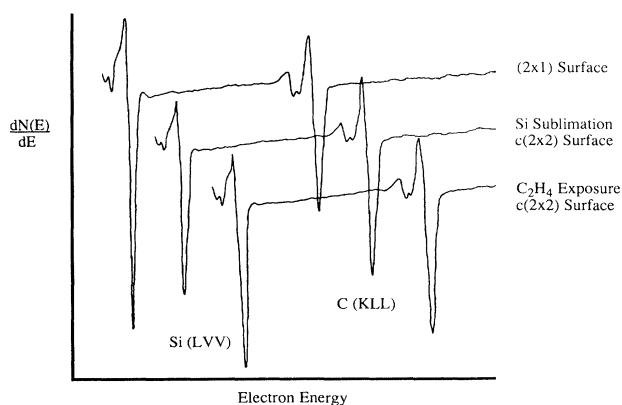

FIG. 5. AES spectra of the β-SiC(100)-(2×1) and c(2×2) surfaces.

TABLE I. Models of β-SiC(100)-$c(2\times2)$ examined using conventional dynamical LEED.

Model	Vertical height range[a,b]	Optimized vertical height	Dimer length range[a]	Optimized dimer length	Pendry R factor
		$c(2\times2)$ via C_2H_4 exposure			
Staggered Si dimers	1.0–1.6		2.15–3.00		c
Staggered C dimers	1.0–1.6	1.32	1.20–1.60	1.46	0.31
Si in C hollows	0.0–1.4	0.77			0.35
C in Si hollows	0.0–1.4	0.20			0.28
Si in C bridges	0.0–1.4	0.60			0.36
C in Si bridges	0.0–1.4	0.36			0.33
C_2 in Si bridges	1.0–2.0	1.62	1.13–1.43	1.26	0.24
		$c(2\times2)$ via Si sublimation			
Staggered Si dimers	1.0–1.6		2.15–3.00		c
Staggered C dimers	1.0–1.6	1.23	1.20–1.60	1.32	0.32
Si in C hollows	0.0–1.4	0.89			0.36
C in Si hollows	0.0–1.4	0.33			0.35
Si in C bridges	0.0–1.4	0.38			0.34
C in Si bridges	0.0–1.4	0.34			0.36
C_2 in Si bridges	1.0–2.0	1.62	1.13–1.43	1.25	0.27

[a]All heights and lengths are in angstroms (Å).
[b]The vertical height is the distance between the first and second atomic layers, with the second layer in its bulklike position.
[c]For the staggered Si dimer model, no R factor minimum was found within the explored ranges.

duced by C_2H_4 exposure, TLEED results showed no significant changes from the conventional dynamical LEED results previously discussed [Fig. 6(a)]. Tensor LEED gave a 2% contraction (0.02 Å) in the second- to third-layer interatomic distance, although this change is well within the uncertainty of the analysis (approximately 0.05 Å). The optimized muffin-tin zero in this case was at -9 ± 1 eV.

For the Si sublimation $c(2\times2)$ data, TLEED results suggested the formation of weak second-layer silicon dimers [Fig. 6(b)]. By allowing second-layer relaxation, the R factor was lowered from 0.27 to 0.22. In this case the optimized muffin-tin zero was at -11 ± 1 eV. This weak silicon dimer has a bond length of 2.71 Å, which is considerably longer than dimers found on the Si(100)-(2×1) surface (2.47 Å).[17] However, this long silicon dimer bond length results in a C—C bond distance of 1.31 Å,

which suggests the surface carbons are sp^2 hybridized. Assuming the C_2 groups to be double bonded, this leaves the surface carbon with the sp^2 dangling bond. Our calculated Si—C distance of 1.93 Å agrees well with the bulk Si—C bond distance of 1.89 Å. This calculated configuration results in a C—C—Si bond angle of 124° vs 120° for ideal sp^2 carbon. Hence, out model of C_2 groups in bridging sites would appear to be able to exist without a high degree of strain. This model of bridging C_2 groups is also favored by total-energy calculations of Badziag.[18] However, that study and the present results differ in a number of ways. Firstly, the two studies return somewhat different bond lengths for the C_2 groups. In addition, the degree of dimerization observed in the second layer is different, with the total-energy study consistently returning shorter Si—Si bond lengths. This may be an artifact of the computational scheme employed by

TABLE II. Models of β-SiC(100)-$c(2\times2)$ examined using tensor LEED.

Model	Optimized vertical height[a,b]	Optimized C—C bond length[a]	Pendry R factor
	$c(2\times2)$ via C_2H_4 exposure		
Staggered C dimers	1.32	1.46	0.31
C_2 in Si bridges	1.62	1.25	0.24
	$c(2\times2)$ via Si sublimation		
Staggered C dimers	1.23	1.32	0.32
C_2 in Si bridges	1.60	1.31	0.22

[a]All heights and lengths are in angstroms (Å).
[b]The vertical height is the distance between the first and second atomic layers, with the second layer in its bulklike position.
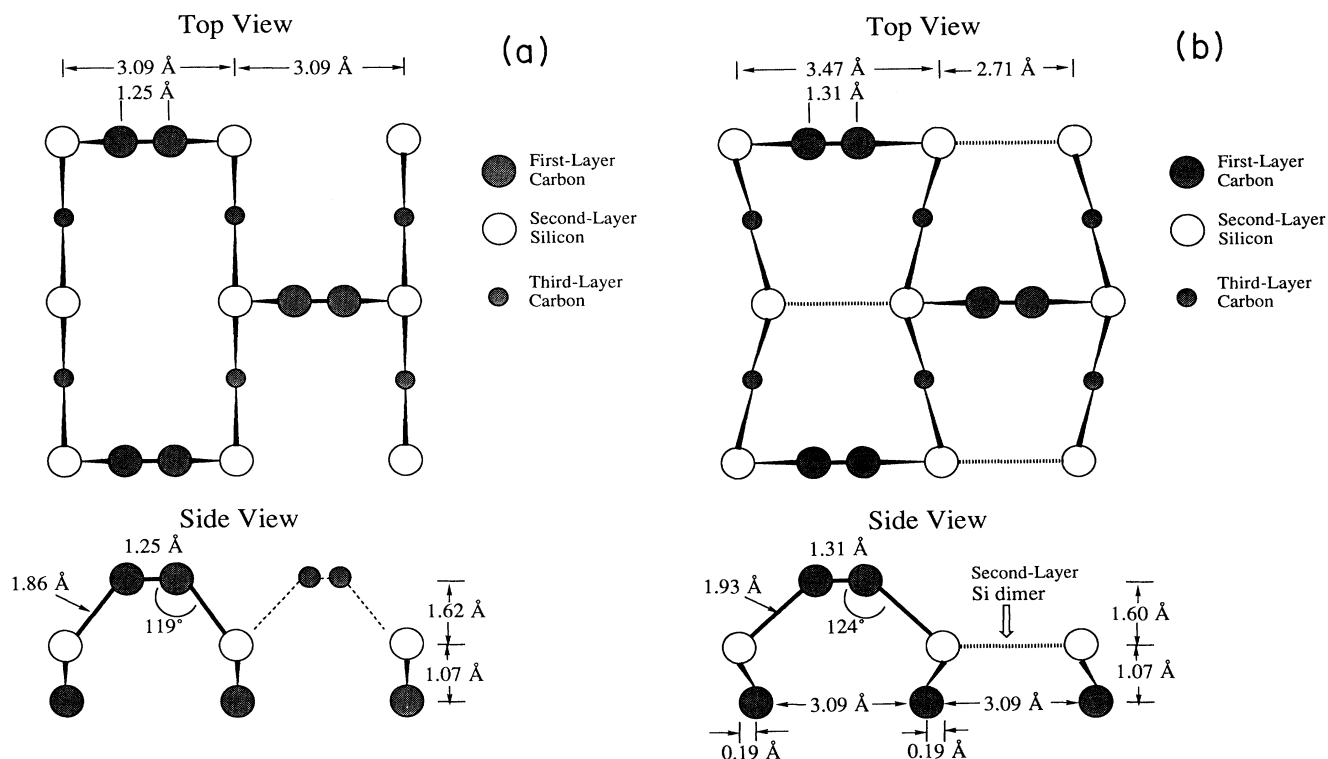
FIG. 6. The best-fit structure for the c(2×2) surface produced by (a) C_2H_4 exposure and (b) Si sublimation.

Badziag. In addition, it should be remembered that LEED is least sensitive to motions parallel to the surface plane, and hence these bond lengths are less well optimized in a LEED study. A full explanation of the subsurface geometry must await future study.

The fact that the Si sublimation and C_2H_4 exposure I-V data sets gave somewhat different surface structures by TLEED suggests that hydrogen plays a role in the c(2×2) surface formed by C_2H_4 exposure. We propose that hydrogen, released by the thermal decomposition of C_2H_4 at 1125 K, could be bonding to surface silicon and/or carbon atoms. These could explain the apparent lack of silicon dimer formation in the second atomic layer of the c(2×2) surface formed by C_2H_4 exposure.

Tensor LEED calculations showed no significant differences from the conventional dynamical LEED results for the staggered carbon dimer model suggested by Bermudez and Kaplan.[19] The optimized R factors for this model, listed in Table II, are significantly higher than those found for the bridging C_2 model. As shown in Fig. 4(a), the staggered carbon dimer model requires significant distortion in the sp^3 bonding of the silicon atoms in the second atomic layer. Badziag's total-energy calculations have predicted the staggered carbon dimer geometry to have substantially higher energy than the bridging C_2 groups model.[18]

VI. CONCLUSIONS

Dynamical LEED I-V analysis of the β-SiC(100)-c(2×2) surface showed the surface to be terminated with a staggered array of C_2 groups in silicon bridge sites. Weak silicon dimer bonds were found in the second atomic layer of the c(2×2) surface produced by silicon sublimation, but not in the c(2×2) surface produced by C_2H_4 exposure. We propose that hydrogen, released by the decomposition of C_2H_4, saturated surface dangling bonds and suppressed silicon dimer function.

ACKNOWLEDGMENTS

*Present address: Department of Physics, University of Maryland Baltimore County, Catonsville, MD 21228.

[1] M. Dayan, J. Vac. Sci. Technol. A **4**, 38 (1986).

[2] S. Adachi, M. Mohri, and T. Yamashina, Surf. Sci. **169**, 479 (1985).

[3] L. Muehlhoff, W. J. Choyke, M. J. Bozack, and J. T. Yates, Jr., J. Appl. Phys. **60**, 2842 (1986).

[4] R. Kaplan, Surf. Sci. **215**, 111 (1989).

[5] S. Hara, W. F. J. Slijkerman, J. F. van der Veen, I. Ohdomari, S. Misawa, E. Sakuma, and S. Yoshida, Surf. Sci. **231**, L196 (1990).

[6] R. Kaplan and T. M. Parrill, Surf. Sci. **165**, L45 (1986).

[7] C. S. Chang, N. J. Zheng, I. Tsong, Y. C. Wang, and R. F. Davis, J. Am. Ceram. Soc. **73**, 3264 (1990).

[8] M. Dayan, J. Vac. Sci. Technol. A **3**, 361 (1985).

[9] J. A. Powell, L. G. Matus, and M. A. Kuczmarski, J. Electrochem. Soc. **134**, 1558 (1987).

[10] P. J. Rous, M. A. Van Hove, and G. A. Somorjai, Surf. Sci. **226**, 15 (1990).

[11] M. A. Van Hove and S. Y. Tong, *Surface Crystallography by LEED,* Springer Series in Chemistry Physics Vol. 2 (Springer, Berlin, 1979).

[12] P. J. Rous, D. Jentz, D. J. Kelly, R. Q. Hwang, M. A. Van Hove, and G. A. Somorjai, in *The Structure of Surfaces-III,* Proc. ICSOS-III, edited by S. Y. Tong, M. A. Van Hove, K. Takayanagi, and X. D. Xie (Springer-Verlag, Berlin, 1991, in press), p. 432.

[13] A. Wander, M. A. Van Hove, and G. A. Somorjai, Phys. Rev. Lett. **67**, 626 (1991).

[14] J. Yoshinobu, H. Tsuda, M. Onchi, and M. Nishijima, J. Chem. Phys. **87**, 7332 (1987).

[15] V. M. Bermudez, J. Appl. Phys. **66**, 6084 (1989).

[16] B. Jørgensen and P. Morgan, J. Vac. Sci. Technol. A **4**, 1701 (1986).

[17] B. W. Holland, C. B. Duke and A. Paton, Surf. Sci. **140**, L269 (1984).

[18] P. Badziag, Phys. Rev. B **44**, 11 143 (1991).

[19] V. M. Bermudez and R. Kaplan, Phys. Rev. B **44**, 11 149 (1991).